metal complexes including Cu. They used a self-consistent charge iteration procedure to refine Coulomb integrals. We omitted that procedure. While we employed the simplest assumption of direct proportionality of resonance integrals to an average of Coulomb integrals times overlap, Zerner and Gouterman used a more sophisticated relationship. Our extended Hückel energy levels for porphine (Figure 3) show a_{1u} as the HOMO with a_{2u} just below. Both are π orbitals. In the energy level scheme obtained by Zerner and Gouterman these levels are reversed. We agree on e_g as the porphine LUMO. Their HOMO–LUMO gap is about 2 eV compared to 1.49 eV from our results. More serious differences occur in comparisons of the energy level pattern for the Cu^{2+} complex of porphine. We found e_g (π) as the singly occupied HOMO of the complex with b_{1g} (σ) vacant above. Zerner and Gouterman show b_{1g} as the singly occupied HOMO with e_g as the LUMO. Both results are consistent with ESR data that has been interpreted as indicating that the odd electron resides primarily on the metal.[29]

Conclusions

On the basis of simple Hückel results it was previously concluded that B_8S_{16} would form much weaker complexes than would porphine and this conclusion is reinforced by extended Hückel calculations that do not include d AOs on the sulfur atoms. However, inclusion of sulfur d AOs changes the composition of the extended Hückel MOs and the pattern of the energy levels and leads to the prediction that the B_8S_{16} complex with Cu^{2+} might be about as stable as the porphine complex. Unfortunately, this conclusion depends on the magnitude of value chosen for the sulfur 3d AO Coulomb integral. Therefore, without a more specific basis for the selection of this parameter, reliable stability predictions for this system are not likely to result from further semiempirical calculations. We were surprised at the importance of the sulfur d AOs although their significance has been noted in other work.[20,21] Because of the consequences of sulfur d AO participation in the electronic structure of B_8S_{16}, this compound differs from the porphine dianion by more than a mere six π electrons. Ligand–metal bonding in both kinds of planar macrocyclic complexes **1** and **2**, as well as that in the tetrathia ether complex **6**, results mainly from a MO of b_{1g} symmetry in which the central-atom $d_{x^2-y^2}$ AO combines in phase with p AOs on the four ligand binding sites.

Registry No. **1**, 73825-17-9; $Cu^{2+}B_8S_{16}$, 83897-43-2; porphine dianion, 30882-36-1; porphine dianion, copper(2+) complex, 13007-96-0.

(29) E. M. Roberts and W. S. Koski, *J. Am. Chem. Soc.*, **82**, 3006 (1960).

Contribution from the Department of Chemistry, Wright State University, Dayton, Ohio 45435

EPR Studies of Cobalt–Dioxygen Complexes Containing Linear, Pentadentate Keto Iminato Ligands

MICHAEL D. BRAYDICH, JOHN J. FORTMAN, and SUE C. CUMMINGS*

Received March 23, 1982

The oxygen adducts of a series of pentacoordinate (keto iminato)cobalt(II) complexes, Co(acacDPT)·O_2, Co(benacDPT)·O_2, Co(tfacDPT)·O_2, Co(acacMeDPT)·O_2, Co(benacMeDPT)·O_2, Co(tfacMeDPT)·O_2, Co(benacPhDPT)·O_2, and Co(tfacPhDPT)·O_2, have been investigated by using EPR spectral techniques. EPR studies were conducted under four sets of conditions in order to provide insight into the interaction of cobalt with dioxygen and to learn if there were any substituent effects. The presence of eight hyperfine lines in both the solution and frozen-glass spectra confirms the formation of 1:1 adducts in all cases. Comparison of the anisotropic coupling constants suggests that the different central amine substituents modify electron density on the cobalt ion through σ effects, while the substituents derived from the β-diketone moiety change electron density via π interactions. Evidence obtained from variable-temperature isotropic spectra and overlapping anisotropic spectra for several of the adducts suggests the existence of two isomers. Time decay and reversibility experiments indicate that the adducts may decay through an oxy-bridged dimer intermediate. This work culminated with the isolation and characterization of the oxygen adduct of Co(benacMeDPT). The IR spectrum of the solid reveals an O–O stretching vibration at 1150 cm^{-1}, consistent with a monomeric adduct. Deoxygenation of the sample results in some irreversible oxidation.

Introduction

Recently we reported the synthesis and characterization of Ni(II), Cu(II), and Co(II) complexes with pentadentate keto iminato ligands formed from the condensation of various β-diketones and triamines.[1] The Co(II) derivatives are of special interest because of their ability to undergo reversible oxygenation.[2,3] Dioxygen adducts of cobalt(II) complexes containing tetradentate ligands have been studied and reviewed extensively.[4-7] In such systems, oxygen binding is generally accompanied by binding of a Lewis base in the coordination site trans to the dioxygen, which gives rise to six-coordinate adducts. The complexes can be viewed as Co(III)–O_2^- species, where the extent of electron transfer from cobalt to oxygen depends on the nature of the in-plane ring substituents and axial bases.

The oxygen adducts of cobalt(II) complexes containing pentadentate ligands have received much less study, even though these systems eliminate the need for addition of an external Lewis base in order to form a six-coordinate dioxygen adduct. Those reports that have appeared in the literature have

(1) Chen, Y.-Y.; Chu, D. E.; McKinney, B. D.; Willis, L. J.; Cummings, S. C. *Inorg. Chem.* **1981**, *20*, 1885, 3582.
(2) Braydich, M. D. M.S. Thesis, Wright State University, Dayton, OH, Dec 1978.
(3) Braydich, M. D.; Fortman, J. J.; Cummings, S. C. "Abstracts of Papers", 11th Central Regional Meeting of the American Chemical Society, Columbus, OH, May 1979.
(4) Wilkins, R. G. *Adv. Chem. Ser.* **1971**, *No. 100*, 111.
(5) McLendon, G.; Martell, A. E. *Coord. Chem. Rev.* **1976**, *19*, 1.
(6) Jones, R. D.; Summerville, D. A.; Basolo, F. *Chem. Rev.* **1979**, *79*, 139.
(7) Smith, T. D.; Pilbrow, J. R. *Coord. Chem. Rev.* **1981**, *39*, 295.

0020-1669/83/1322-0484$01.50/0

dealt with only pentadentate Schiff base ligands derived from various salicylaldehydes and triamines.[8-13] The EPR studies reported herein provide new data on the cobalt–dioxygen interaction in pentacoordinate (keto iminato)cobalt(II) complexes. The general structure and abbreviations for the eight new complexes studied are shown in I. Unlike oxygenation

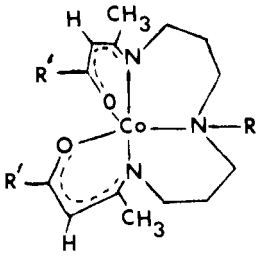

Ia:	$R = H, R' = CF_3$	Co(tfacDPT)
b:	$R = CH_3, R' = CF_3$	Co(tfacMeDPT)
c:	$R = C_6H_5, R' = CF_3$	Co(tfacPhDPT)
d:	$R = H, R' = C_6H_5$	Co(benacDPT)
e:	$R = CH_3, R' = C_6H_5$	Co(benacMeDPT)
f:	$R = C_6H_5, R' = C_6H_5$	Co(benacPhDPT)
g:	$R = H, R' = CH_3$	Co(acacDPT)
h:	$R = CH_3, R' = CH_3$	Co(acacMeDPT)

of square-planar tetradentate complexes, the reaction of dioxygen with the pentacoordinate (iminato)cobalt(II) complexes may produce geometric isomers in which the dioxygen moiety is coordinated either cis or trans to the tertiary nitrogen atom. The EPR studies reported here were undertaken to provide insight into the isomer question and to study the effects of chelate ring substituents.

Experimental Section

Materials. Cobalt complexes were prepared as described elsewhere.[1] Analytical reagent grade toluene (Mallinckrodt) and reagent grade methylene chloride (Fisher) were refluxed for 1 h over CaH_2 and P_4O_{10}, respectively, before distillation under dry nitrogen. Both solvents were degassed by using the freeze–pump–thaw technique and stored under a nitrogen atmosphere in a Vacuum Atmospheres glovebox equipped with Dri-Train until used. *N*-(*p*-Methoxybenzylidene)-*p*-butylaniline (Eastman) was degassed and then used as received. Research grade oxygen, 99.9%, was obtained from Matheson and was used as supplied.

Physical Measurements. A Perkin-Elmer Model 457 infrared spectrophotometer was used to record IR spectra of all samples, and magnetic susceptibility measurements were determined by the Faraday technique using an Alfa electromagnet equipped with 4-in. constant-force pole caps. Measured susceptibilities were corrected for ligand contributions by using Pascal's constants.

EPR Instrumentation. EPR spectra were obtained on a Varian E-104A Century Line Spectrometer equipped with a quartz liquid-nitrogen-insert dewar for obtaining frozen-glass spectra. Low-temperature solution spectra were obtained with the Varian variable-temperature control apparatus. Temperatures at the end of the sample tubes were measured with a thermocouple (±2 K). Spectra were recorded in the X band at a frequency of ~9.1 GHz. The magnetic field was calibrated with a Hewlett-Packard Model HX 532B frequency meter. Field corrections for samples were made with DPPH as the external standard.

EPR Sample Preparation. Typically, a 3.5-mg sample of the complex was weighed in air and placed in a small vial. The sample vial was placed in the port of the glovebox and evacuated for a minimum of 1 h to remove adsorbed oxygen and water from the sample. The sample bottle was taken into the box and covered with a septum, and the appropriate amount of solvent (2:1 v/v mixture of toluene/methylene chloride) needed to give a $\sim 10^{-2}$ *m* solution was syringed into the sample bottle (solubility limits required the use of $\sim 10^{-3}$ *m* for Co(benacDPT) and Co(benacMeDPT)). Approximately 0.3 mL of complex solution was then syringed into a 3-mm-o.d. quartz EPR tube. The tube was sealed with a septum, removed from the glovebox, and placed in the appropriate low-temperature slush bath until EPR measurements were undertaken.

Isotropic Spectra. Isotropic solution spectra of the oxygen adducts were obtained at four temperatures (0, −23, −45, and −63 °C) by using the Varian variable-temperature control apparatus. Prior to the measurements, each sample was allowed to equilibrate for at least 15 min in ice water (0 °C) or in the required low-temperature liquid-nitrogen slush bath (−23 °C, carbon tetrachloride; −45 °C, chlorobenzene; −63 °C, chloroform). While in the slush, each sample was oxygenated by bubbling O_2 through the solution for 30 s, followed by shaking. At this point the external standard, DPPH, contained in a sealed melting point capillary tube, was placed in the sample tube and the sample was resealed with the septum. Solvent wetting of the sides of the EPR tube prevented the standard from falling to the bottom of the tube. Since DPPH obscures part of the pattern for the oxygen adduct, the DPPH was not tapped to the bottom of the EPR tube until standardization of the magnetic field was required. Two spectra were recorded for each sample, one with a scan width of 400 g and the other at 100 g. The latter-width spectrum was used to calculate *g* values and hyperfine splitting constants. Three samples of each complex were run to check the reproducibility of the spectral parameters. In all cases the values were reproducible to ±0.5 G for hyperfine splitting constants and ±0.001 G for *g* values.

Anisotropic Spectra. Frozen-glass spectra were obtained at −196 °C with use of a liquid-nitrogen-insert dewar that was positioned in the cavity. Samples removed from the glovebox were placed in a dry ice–acetone bath and allowed to equilibrate for 15 min. The same oxygenating procedure was used as for the isotropic samples. Two spectra were recorded for each sample, one with a scan width of 1000 G and the other at 100 G. When the DPPH was needed, the sample was removed from the dewar and allowed to thaw in the dry ice–acetone bath. The standard was then tapped to the bottom, and the EPR tube was returned to the dewar for measurements. The procedure used for orienting samples in nematic liquid-crystal glasses was similar to that described by Fackler et al.[14]

Reversibility Measurements. These studies were performed at three temperatures, 0, −23, and −45 °C. Samples were prepared by the same procedure outlined for isotropic solution studies. After the eight-line isotropic pattern was recorded, the spectrometer was returned to the standby mode and a capillary tube attached to a dry-nitrogen source was inserted to the bottom of the EPR tube. A slow flow of prepurified nitrogen gas was bubbled through the solution to displace both chemically bound dioxygen and the oxygen dissolved in solution. After 15 min the capillary tube was removed and the EPR tube was shaken to force all of the solution to the bottom of the tube. The spectrum was again recorded. If an isotropic signal persisted, the capillary tube was reinserted and nitrogen was bubbled through the solution for an additional 15 min. This procedure was repeated until a straight line was observed (loss of the isotropic signal). The sample was removed from the cavity, reoxygenated for 30 s in the appropriate slush bath, and returned to the cavity. Once again the spectrum of the sample was recorded. If the sample did not give the typical isotropic pattern, it was removed and reoxygenated for an additional 30 s and the spectrum recorded. During this experiment, the gain, modulation, and power settings remained the same for the initial oxygenation, deoxygenation, and reoxygenation steps.

Time-Decay Measurements. Data were recorded at two temperatures, 0 and −23 °C. For comparison of the signals of the various samples, the gain, modulation, and power settings were held constant throughout each experiment. Thus, differences in signal intensities reflect varying degrees of oxygenation of the cobalt complexes. Measurements were begun at 0 °C with the cobalt complex that gave the weakest isotropic signal, ensuring a well-resolved spectrum for that sample as well as those more highly oxygenated. Cobalt complexes used were Co(acacDPT), Co(tfacDPT), Co(benacDPT), and Co(benacMeDPT). A typical sample was prepared by placing ap-

(8) Tovrog, B. S.; Drago, R. S. *J. Am. Chem. Soc.* **1974**, *96*, 6765.
(9) Niswander, R. H.; St. Clair, A. K.; Edmondson, S. R.; Taylor, L. T. *Inorg. Chem.* **1975**, *14*, 478.
(10) Hoffman, B. M.; Szymanski, T.; Basolo, F. *J. Am. Chem. Soc.* **1975**, *97*, 673.
(11) Niswander, R. H.; Taylor, L. T. *Inorg. Chem.* **1976**, *15*, 2360.
(12) Tovrog, B. S.; Kitco, D. J.; Drago, R. S. *J. Am. Chem. Soc.* **1976**, *98*, 5144.
(13) Niswander, R. H.; Taylor, L. T. *J. Magn. Reson.* **1977**, *26*, 491.
(14) Fackler, J. P.; Levy, J. D.; Smith, J. A. *J. Am. Chem. Soc.* **1972**, *94*, 2436.

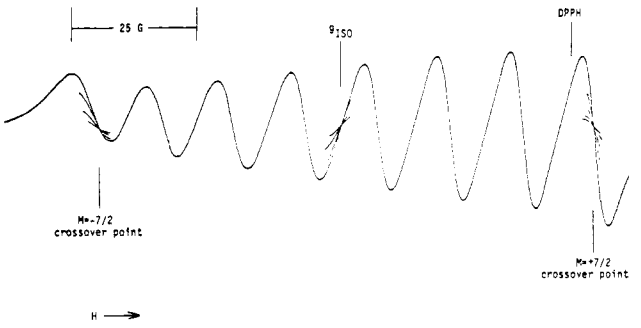

Figure 1. Isotropic solution spectrum of Co(acacDPT)·O_2 at −23 °C in 2:1 v/v toluene/methylene chloride. Crossover points result from rescan of the spectrum at successively lower gain and modulation settings.

proximately 2.3 mg of complex, weighed in air, into a 10-mL volumetric flask. The sample was placed in the entry port of the glovebox and evacuated for a minimum of 1 h. Once in the glovebox, the volumetric flask was capped with a septum and filled with a 2:1 v/v solution of toluene and methylene chloride. Solution concentrations were 1.0×10^{-3} *m*. The filled EPR tubes were removed from the glovebox, degassed three times, and submerged into the appropriate slush bath to equilibrate. After 10 min, O_2 was added to the system at atmospheric pressure. The sample was capped with a septum and inverted three times to allow mixing of the solution with the oxygen. The sample was then placed in the cavity of the spectrometer with the temperature-control apparatus already set to the desired temperature. The first EPR scan was recorded 8 min after oxygenation. Additional scans were recorded at 15-min intervals until the isotropic signal vanished.

Isolation of the Co(benacMeDPT) Oxygen Adduct. A 0.2-g sample of Co(benacMeDPT) was placed in a 75-mL round-bottom flask. The sample was evacuated for 1 h in the entry port. In the glovebox, 4 mL of toluene/methylene chloride solvent was added to the sample (approximately 10^{-1} *m* concentration). Capped with a ground-glass stopper, the sample was removed from the glovebox and placed in a dry ice–acetone bath. After 2 min of oxygenation, a black precipitate was isolated by filtration in air at room temperature. (Filtering in the air at reduced temperatures is not advised, because water condenses on the sample.) The black solid was washed with 2 mL of hexane and air-dried for 3 min. Since the sample begins to change color from black to light brown after 20–30 min, an IR spectrum was immediately recorded after the 3-min drying period. Using the same IR sample, we recorded a second spectrum 15 min later. The remainder of the black precipitate was divided into two portions. One was dried in a desiccator under vacuum for $^1/_2$ h, and the other was air-dried for $^1/_2$ h. After the initial drying period, an IR spectrum of the air-dried sample was recorded. The remainder of the air-dried sample was placed in the entry port, evacuated overnight, and stored in the glovebox. Following the initial vacuum-drying period in the desiccator, the second sample was evacuated for 1 h in the entry port. An IR sample was prepared in the glovebox and the IR spectrum recorded. The remainder of the vacuum-dried sample was also stored in the glovebox.

Additional characterization of the dried samples included magnetic susceptibility measurements, EPR isotropic solution spectra at −23 °C, and frozen-glass spectra. Also, reversibility measurements were recorded for the vacuum-dried sample at −23 °C.

Results

Four types of EPR studies on the oxygen adducts were completed. These included (1) isotropic solution spectra as a function of temperature, (2) frozen-glass spectra, (3) reversible oxygenation studies in solution, and (4) time-decay measurements.

The EPR parameters calculated from the isotropic solution spectra obtained at four different temperatures are listed in Table I. Also reported are the color changes observed when solutions of the cobalt(II) complexes are oxygenated. The intensity of the colors provides a visual measure of the degree of oxygenation. The solution spectrum of Co(acacDPT)·O_2 is typical of the eight-line patterns observed for all of the

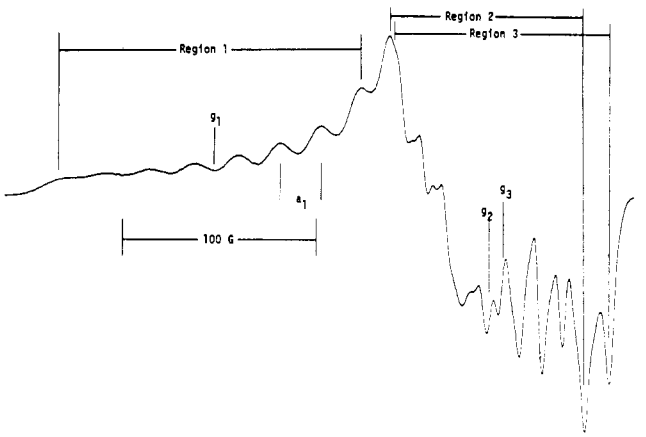

Figure 2. Frozen-glass spectrum of Co(benacMeDPT)·O_2 at −196 °C, illustrating the three spectral regions.

oxygen adducts and is illustrated in Figure 1. Also illustrated here is the "reduction method" used to pinpoint g_{iso} values that involved scanning through the signal three or four times, each time at a lower setting on the gain and modulation dials, to give a reduced signal amplitude. Consecutive reductions aided in determining the crossover points, which are labeled in Figure 1.

Anisotropic spectra were obtained by freezing solutions of the oxygen adducts in 2:1 v/v toluene/methylene chloride to −196 °C. The frozen-glass spectrum of Co(benacMeDPT)·O_2, shown in Figure 2, is typical of spectra obtained for all of the frozen oxygen adducts. The three anisotropic spectral regions have been identified by adopting the method of Taylor and Niswander.[13,15] Cutoffs used for the three regions are also shown in Figure 2. Some support for boundaries of the regions has been obtained from our nematic liquid-crystal studies, which resulted in the disappearance of all of the lines in region 1 (the parallel region) when the oriented sample was rotated by 90°. Boundaries within the perpendicular (high-field) region are less firm. Indeed, a recent computer analysis of Taylor's spectra suggests that the magnitudes of *A* values read from the actual spectra may be in error.[7] Since we are most interested in trends in *A* values rather than absolute magnitudes, we have chosen to follow Taylor's procedures so that some comparisons can be made between the related salicylidene and keto imine complexes. The EPR parameters calculated from the frozen-glass spectra obtained in the current study are reported in Table II.

The relative ability of the cobalt complexes to act as reversible oxygen carriers was determined by monitoring the loss of the eight-line isotropic signal after the molecularly bound dioxygen had been displaced by nitrogen gas followed by its reappearance at similar intensities after reoxygenation. Highly reversible behavior is depicted in the spectra of Co(benacMeDPT)·O_2 at −23 °C shown in Figure 3. Results of similar studies on six samples are reported in Table III.

The rate of decay of four oxygen adducts could be measured at temperatures of 0 and −23 °C. The other samples either failed to give an isotropic signal at the higher temperature or decayed too rapidly for meaningful data collection. The time-decay spectrum of Co(tfacDPT)·O_2 at −23 °C is shown in Figure 4 and is typical of the type of data collected. Variations in signal intensities for the different complexes are representative of different degrees of reactivity with dioxygen. Relative signal intensities for each of the adducts studied are reported in Table IV as both percentage decrease and ln (percent). The latter data were used to construct the plots shown in Figure 5.

(15) Taylor, L. T., private communication, Aug 1978.

Table I. Variable-Temperature Isotropic Solution Spectral Parameters for Cobalt(II)–Oxygen Adducts

oxygen adduct	isotropic parameters and color[a,b]	temp, °C 0	−23	−45	−63
Co(acacDPT)·O_2	*g*	2.034	2.034	2.034	2.033
	a	14.8	14.8	14.2	13.1
	A	14.0	14.0	13.5	12.4
	color	lt r-brn	lt r-brn	dk r-brn	dk r-brn
Co(benacDPT)·O_2	*g*	2.034	2.034	2.034	*c*
	a	14.4	14.4	14.3	
	A	13.7	13.7	13.6	
	color	gold	gold	dk amber	dk amber
Co(tfacDPT)·O_2	*g*	2.031	2.031	2.032	2.031
	a	14.5	14.4	14.0	13.5
	A	13.7	13.6	13.3	12.8
	color	dk green	dk red	dk red	dk red
Co(acacMeDPT)·O_2	*g*	2.028	2.029	2.030	2.031
	a	14.6	14.6	14.4	14.3
	A	13.8	13.9	13.6	13.6
	color	lt r-brn	lt r-brn	dk r-brn	dk r-brn
Co(benacMeDPT)·O_2	*g*	2.027	2.028	2.029	*c*
	a	14.3	13.9	14.0	
	A	13.5	13.2	13.3	
	color	gold	gold	dk amber	dk amber
Co(tfacMeDPT)·O_2	*g*	*d*	*d*	2.025	2.024
	a			12.4	12.4
	A			11.7	11.7
	color	green	dk green	dk green	dk red
Co(benacPhDPT)·O_2	*g*	*e*	*e*	*e*	*d*
	a				
	A				
	color	lt amber	lt amber	lt amber	lt amber
Co(tfacPhDPT)·O_2	*g*	*e*	*e*	*e*	*d*
	a				
	A				
	color	lt amber	lt amber	lt amber	lt amber

[a] Error limits based on the reproducibility of repeated trials: *g* value, ±0.001; *a* (absolute value of the hyperfine splitting constant in gauss), ±0.2; *A* (absolute value of the hyperfine coupling constant in 10^{-4} cm^{-1}), ±0.2. [b] Color of the oxygen adduct in solution; dk, dark; lt, light; r-brn, red-brown. [c] Broadening of spectral lines prevented calculation of parameters. [d] Poorly resolved spectrum prevented calculation of parameters. [e] No EPR signal was observed.

Table II. Frozen-Glass Spectral Parameters[a] for Cobalt(II)–Oxygen Adducts

oxygen adduct	g_1 (±0.001)	g_2 (±0.001)	g_3 (±0.001)	a_1[b] (±0.5)	a_2[b] (±0.2)	a_3[b] (±0.2)	A_1[c] (±0.5)	A_2[c] (±0.2)	A_3[c] (±0.2)
Co(acacDPT)·O_2	2.091	2.005	2.000	24.0	12.5	14.5	23.4	11.7	13.5
Co(benacDPT)·O_2	2.094	2.003	2.000	20.0	12.5	12.9	19.5	11.7	12.0
Co(tfacDPT)·O_2	2.096	2.001	1.998	23.8	12.9	13.7	23.3	12.0	12.8
Co(acacMeDPT)·O_2	2.101	2.005	2.000	23.2	12.9	14.0	22.7	12.1	13.1
Co(benacMeDPT)·O_2	2.097	2.004	1.999	22.1	13.0	14.1	21.6	12.1	13.1
Co(tfacMeDPT)·O_2	2.088	2.003	1.999	18.9	12.5	13.9	18.4	11.7	13.0
Co(benacPhDPT)·O_2	2.101	2.002	1.997	27.0	14.9	16.8	26.5	13.9	15.7
Co(tfacPhDPT)·O_2	2.086	2.002	1.996	24.1	14.9	16.3	23.5	13.9	15.2

[a] Error limits are based on the reproducibility of repeated trials. [b] Absolute value of hyperfine splitting constant in gauss. [c] Absolute value of hyperfine coupling constant in 10^{-4} cm^{-1}.

Table III. Results of the Reversibility Studies for the Pentacoordinate (Keto iminato)cobalt(II) Complexes

complex	temp., °C 0	−23	−45
Co(acacDPT)	partial	partial	complete
Co(benacDPT)	partial	partial	complete
Co(tfacDPT)	complete	complete	complete
Co(acacMeDPT)	partial	partial	complete
Co(benacMeDPT)	partial	complete	complete
Co(tfacMeDPT)	*a*	complete	complete

[a] Weak signal did not permit testing.

Discussion

The EPR measurements reported here were undertaken to provide insight into the cobalt–dioxygen interaction and to learn if there were any ring substituent effects. The presence of eight hyperfine lines in both the solution and frozen-glass spectra confirms the 1:1 nature of the adducts in all cases.

The frozen-glass spectra are very similar to those reported by Niswander and Taylor for pentacoordinate salicylideneaminato systems.[13] As observed by these authors, we also find that there is poor agreement between experimentally determined g_{iso} and A_{iso} values and those obtained by averaging the anisotropic *g* and *A* parameters. The problem may arise from the presence of geometric isomers in these systems (vide infra) and, in part, from the difficulty in accurately measuring parameters in the perpendicular region (g_2, g_3; A_2, A_3).[7] Still, trends in A_1 values may be considered a reasonably accurate measure of the strength of the cobalt–dioxygen interaction. From the data in Table II we see that both the triamine and β-diketone affect the Co–O_2 interaction, with A_1 values decreasing in the general order PhDPT > DPT > MeDPT and acac > benac > tfac. The first trend can be explained on the basis of inductive effects. The trend parallels the Hammett σ values of the substituent on the tertiary nitrogen, with the

Table IV. Results of the Time-Decay Studies for the Cobalt(II)–Oxygen Adducts

oxygen adduct	rel intens[a,c] 0 °C	rel intens[a,c] −23 °C	% intens[d] 0 °C	% intens[d] −23 °C	ln % 0 °C	ln % −23 °C	time, min
Co(acacDPT)·O_2	2.14 ± 0.04	27.22 ± 0.3	100	100	4.61	4.61	0
	0.22	13.21 ± 0.8	10.3	48.5	2.33	3.88	15
		7.08 ± 1		26.0		3.26	30
		3.50 ± 0.4		12.9		2.56	45
		2.06 ± 0.7		7.6		2.03	60
Co(benacDPT)·O_2	9.32 ± 5	12.41 ± 3	100	100	4.61	4.61	0
	1.46 ± 1	8.89 ± 3	15.7	71.6	2.75	4.27	15
	0.33 ± 0.6	5.56 ± 2	3.5	44.8	1.25	3.80	30
		4.28 ± 2		34.5		3.54	45
		3.43 ± 1		27.6		3.32	60
		2.79 ± 1		22.5		3.11	75
Co(tfacDPT)·O_2	5.79 ± 0.2	16.79 ± 0.03	100	100	4.61	4.61	0
	2.32 ± 0.2	14.37 ± 0.1	40.1	84.7	3.69	4.44	15
	0.86 ± 0.1	11.89 ± 0.3	14.9	70.0	2.70	4.25	30
	0.31	8.99 ± 0.1	5.4	52.9	1.69	3.97	45
		7.40 ± 0.2		43.6		3.78	60
Co(benacMeDPT)·O_2	14.60 ± 1	13.80 ± 0.9[e]	100	100	4.61	4.61	0
	4.55 ± 1	11.29 ± 1	13.1	81.8	3.44	4.40	15
	1.55 ± 0.4	9.61 ± 1	10.3	69.6	2.33	4.24	30
	0.63 ± 0.1	8.16 ± 2	4.3	59.1	1.46	4.08	45
		6.89 ± 2		49.7		3.91	60
		6.19 ± 2		44.8		3.80	75

[a] Determined by using the equation $I \propto Y'_{max}(\Delta H_{pp})^2$, where I = intensity, Y'_{max} = peak-to-peak amplitude, and ΔH_{pp} = peak-to-peak width. [b] Arbitrary units. [c] Error limits were determined by averaging the measurements to arrive at the deviation. [d] Percent intensity based on the first recorded spectrum for each oxygen adduct. [e] Only the $M = -3/2$ to $M = 5/2$ derivative lines were used to calculate the relative intensity, since the remaining lines were off-scale.

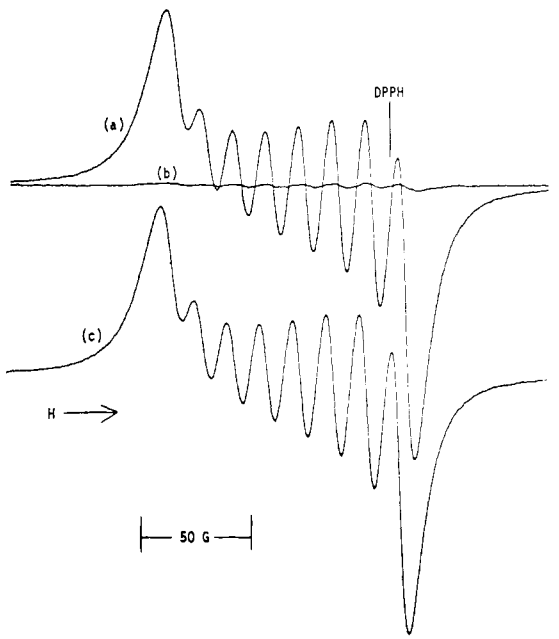

Figure 3. Reversibility spectra for Co(benacMeDPT)·O_2 at −23 °C: (a) oxygenation; (b) deoxygenation; (c) reoxygenation.

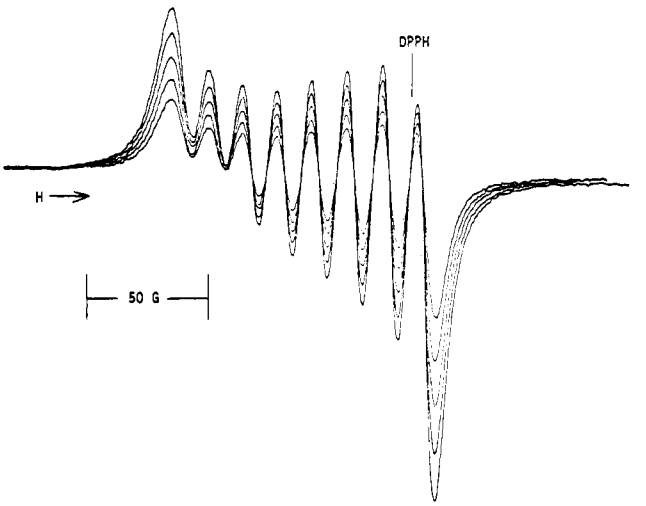

Figure 4. Time-decay spectrum for Co(tfacDPT)·O_2 at −23 °C.

electron-withdrawing phenyl group producing the smallest cobalt–dioxygen interaction (largest A_1 value) and the electron-donating methyl group producing the largest dioxygen bonding interaction (smallest A_1 value). These findings are in agreement with those reported for the salicylideneaminato complexes.[11,13] The trend in A_1 values resulting from substituent changes in the iminato rings is the opposite of what would be predicted on the basis of inductive effects. This may be indicative of a change in π interactions.

Isotropic solution measurements also reflect the substituent effects. In general, a decrease in A_{iso} corresponds to more transfer of unpaired-spin density to dioxygen, which should result in enhanced adduct stability. Thus, at −23 °C, the trend in A_{iso} is Co(acacDPT)·O_2 ≳ Co(acacMeDPT)·O_2 > Co(benacDPT)·O_2 ≳ Co(tfacDPT)·O_2 > Co(benacMeDPT)·O_2 with greatest stability expected for the adduct that contains an electron-donating methyl group on the tertiary nitrogen of the triamine and electron-withdrawing phenyl groups on the keto iminato rings. These observations are borne out by the fact that Co(benacMeDPT)·O_2 is the only adduct that we could isolate in the solid state. The IR spectrum of this black microcrystalline product exhibits a very strong absorption band at 1150 cm^{-1}, which is not present in the spectrum of the five-coordinate precursor. After a 15-min exposure to air, this absorption band disappears, which suggests that the IR-active band is due to the O–O stretching vibration of coordinated dioxygen. Similar band energies for the O–O vibration have been reported for the monomeric dioxygen adducts of several Co(acacen)·B[16] and porphyrin complexes.[17,18] The O–O stretching mode for μ-peroxo Co(III) complexes is invariably

(16) Hoffman, B. M.; Diemente, D. L.; Basolo, F. *J. Am. Chem. Soc.* **1970**, *92*, 61.
(17) Collman, J. P.; Brauman, J. J.; Halbert, T. R.; Suslick, K. S. *Proc. Natl. Acad. Sci. U.S.A.* **1976**, *73*, 3333.
(18) Dey, K. *Z. Anorg. Allg. Chem.* **1970**, *366*, 209.

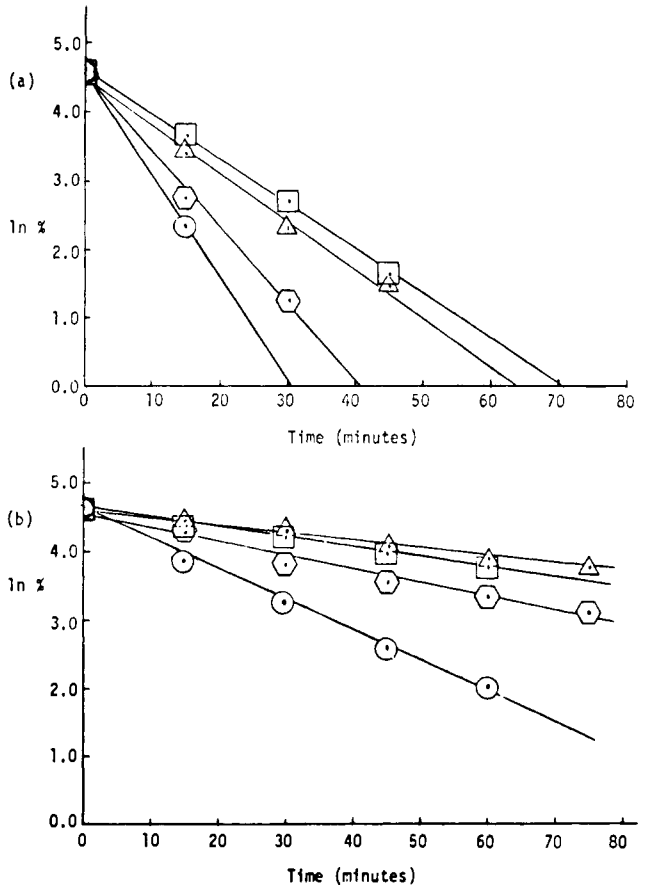

Figure 5. Time-decay curves for Co(acacDPT)·O_2 (○), Co(benacDPT)·O_2 (○), Co(tfacDPT)·O_2 (□), and Co(benacMeDPT)·O_2 (△) at (a) 0 and (b) −23 °C.

observed at lower energies, i.e. 930–800 cm^{-1}.[5,19] The fact that the IR spectrum of the air-exposed sample shows a new band (albeit weak and broad) at 840 cm^{-1} may indicate decomposition via the bridged species. Our studies of solution decay rates (vide infra) also suggest this as a possibility. When the oxygenated black solid is immediately dissolved in degassed solvent, the EPR spectrum obtained is identical with that found for Co(benacMeDPT)·O_2 generated in solution. A magnetic susceptibility measurement on the black solid, which had been vacuum dried (deoxygenated), gave μ_{eff} = 4.2 μ_B, which compares to a moment of 4.5 μ_B for the unoxygenated starting material. From these data we conclude that there is ~15% conversion to an irreversibly oxidized material. Oxidation is more extensive (~50%) when the adduct is allowed to deoxygenate more slowly in air. Both types of dried samples can be reoxygenated in solution; however, the EPR signals obtained are different. The vacuum-dried sample gives isotropic and anisotropic spectra very close to those found for Co(benacMeDPT)·O_2. The spectral line shapes for the isotropic and frozen-glass spectra of the reoxygenated air-dried sample are much different, which suggests the presence of a different EPR-active species.

It is interesting to speculate on the possible existence of isomers from the oxygenation reactions reported here. As can be seen from Figure 6, adduct formation can occur by dioxygen attack either cis or trans to the tertiary nitrogen located in the equatorial plane. Chance favors the cis isomer by 2:1; however, steric and electronic effects of the ring substituents may alter this distribution. Air-drying of the Co(benacMeDPT)·O_2 sample may have selectively destroyed one geometric isomer

(19) Nakamoto, K.; Nonaka, Y.; Ishiguro, T.; Urban, M. W.; Suzuki, M.; Kozuka, M.; Nishida, Y.; Kida, S. *J. Am. Chem. Soc.* **1982**, *104*, 3386.

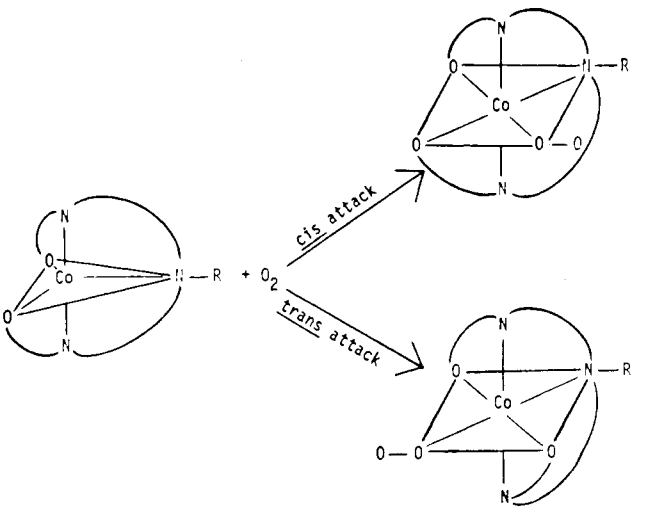

Figure 6. Reaction of dioxygen with a trigonal-bipyramidal cobalt complex leading to a mixture of cis and trans isomers.

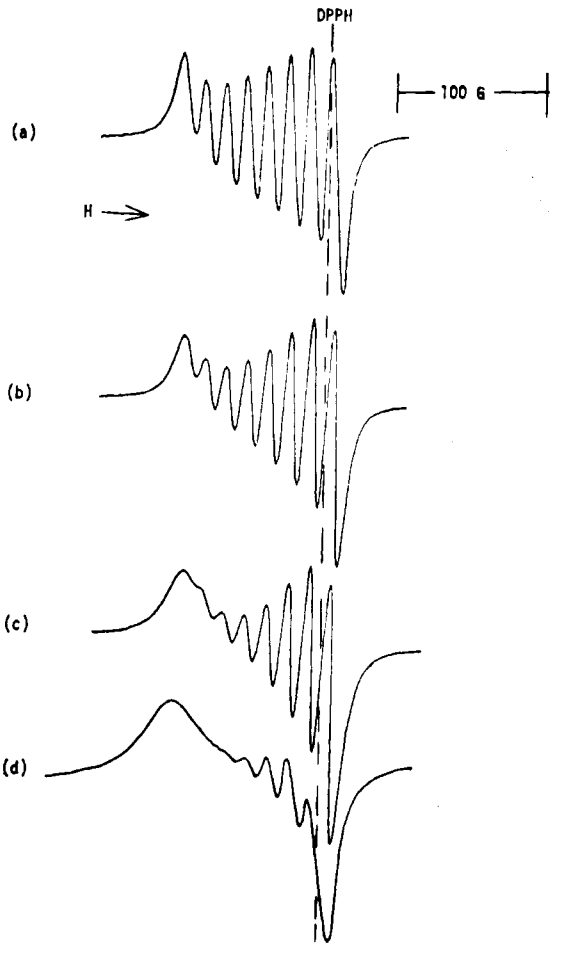

Figure 7. Isotropic solution spectra of Co(benacDPT)·O_2 at (a) 0, (b) −23, (c) −45, and (d) −63 °C, illustrating the effect of temperature.

in the mixture, thus causing significant changes in the EPR spectral patterns of the reconstituted adduct.

The presence of isomers is also suggested by the fact that the isotropic spectral patterns are temperature dependent. Figures 7 and 8 illustrate broadening of the solution spectra of Co(benacDPT)·O_2 and Co(tfacMeDPT)·O_2 as a function of temperature. As the temperature decreases, the EPR signal of an isomer mixture should broaden due to incomplete averaging of the signals from the two isomers, caused by a reduced interconversion rate. When the rate of exchange becomes extremely slow on the EPR time scale, a sharpening

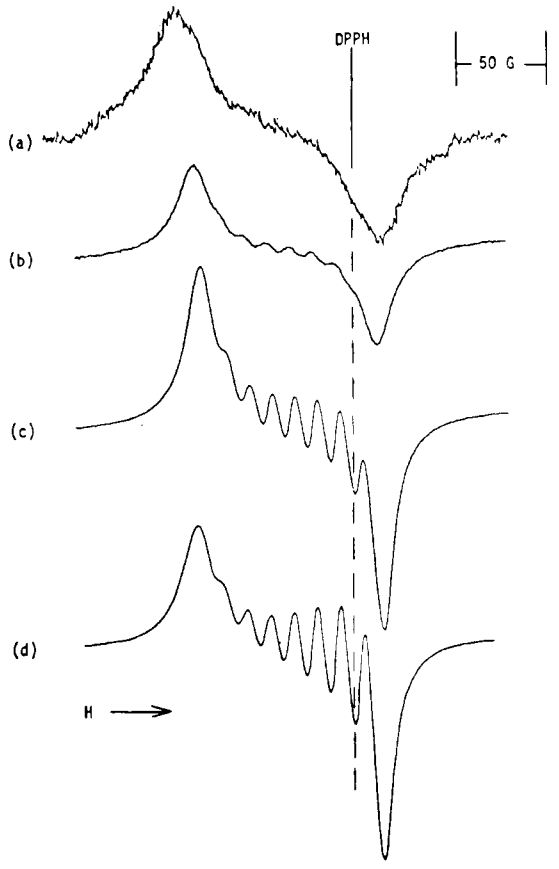

Figure 8. Isotropic solution spectra of Co(tfacMeDPT)·O_2 at (a) 0, (b) −23, (c) −45, and (d) −63 °C, illustrating the temperature-dependent spectral changes.

of spectral patterns should be observed again. Different interconversion energy barriers will influence the exact temperature at which the rate of interconversion is affected. Thus, temperatures of −45 and −63 °C are observed to produce broadening for Co(benacDPT)·O_2 possibly due to slow interconversion of cis and trans isomers, whereas these same temperatures produce a sharp pattern for Co(tfacMeDPT)·O_2, indicating virtually no interconversion or very fast interconversion is taking place. It should be noted that two distinct signals would be observed under conditions of slow exchange only if the isomers resonated at different magnetic fields or had the same g value but different coupling constants, which is unlikely for the cis and trans isomers postulated here. A sharpening of the spectral pattern and reduction in A_{iso} values may be the only indicators of the isomer mixture under conditions of either very fast or very slow exchange.

Results of the reversibility studies, presented in Table III, show that all six complexes exhibit reversible binding to dioxygen at −45 °C; but only Co(tfacDPT)·O_2 loses O_2 reversibly at all three temperatures studied. Perhaps the presence of the strongly withdrawing CF_3 groups retards decomposition of the parent complex during the oxygenation/deoxygenation cycles.

Data from the rate of decay studies, Table IV and Figure 5, show that Co(tfacDPT)·O_2 and Co(benacMeDPT)·O_2 have similar kinetic stabilities at 0 and −23 °C. Therefore, one might anticipate that oxygenation of Co(benacMeDPT) would also be totally reversible at these temperatures. The reduced reversibility of Co(benacMeDPT)·O_2 at 0 °C may be dependent on differences in the isomers present and the nature of the decay mechanism.

In general, an oxygen adduct may be destroyed by at least three mechanisms. First, the adduct could dissociate, reforming the parent complex and releasing dioxygen. Second, the oxygen adduct might combine with another molecule of the parent complex to form an oxy-bridged dimer. Finally, the cobalt and/or ligand might be irreversibly oxidized by the dioxygen to leave only diamagnetic non-EPR-active species in solution. Since oxygenation of our decayed samples does not restore the isotropic spectra in any case, the first mechanism can be eliminated. Support for an oxy-bridged dimer as an intermediate in the decay processs is consistent with the order of decay, i.e., Co(acacDPT)·O_2 > Co(benacDPT)·O_2 > Co(tfacDPT)·O_2 ≃ Co(benacMeDPT)·O_2, since the decay is slowest for the complexes with the bulkiest substituents. If dimer formation were involved in the decay mechanism, steric effects due to phenyl and CF_3 groups might hinder the approach of a second parent molecule necessary to form the oxy bridge. The fact that the oxygen adducts decay by first-order kinetics does not preclude a bimolecular mechanism, since the second species required for bridge formation is EPR inactive. Unfortunately, our attempts to isolate a pure μ-peroxo-bridged dimer or to fully characterize any of the decomposition products have been unsuccessful.

Acknowledgment. S.C.C. gratefully acknowledges financial support of this investigation by the National Institutes of Health, Grant HL 15640, from the Heart, Lung, and Blood Institute. Completion of this work by M.D.B. was made possible through an educational leave assignment from the Air Force Institute of Technology, Wright-Patterson AFB, OH.

Registry No. Co(tfacDPT), 77097-11-1; Co(tfacMeDPT), 77097-12-2; Co(tfacPhDPT), 77097-13-3; Co(benacDPT), 77110-76-0; Co(benacMeDPT), 77097-27-9; Co(benacPhDPT), 77097-28-0; Co(acacDPT), 77097-18-8; Co(acacMeDPT), 77097-19-9; Co(tfacDPT)·O_2, 83947-11-9; Co(tfacMeDPT)·O_2, 83947-12-0; Co(tfacPhDPT)·O_2, 83947-13-1; Co(benacDPT)·O_2, 83947-14-2; Co(benacMeDPT)·O_2, 83947-15-3; Co(benacPhDPT)·O_2, 83947-16-4; Co(acacDPT)·O_2, 83947-17-5; Co(acacMeDPT)·O_2, 83947-18-6.